Comparison of sensitivity and resolution with two marine CSEM exploration methods

David Alumbaugh, Nestor H. Cuevas, Jiuping Chen, Guozhong Gao and James Brady; Schlumberger*

SUMMARY

This paper compares the sensitivity to, and resolution of the properties of a resistive target using marine controlled source electromagnetic measurements, with the frequency domain horizontal source-receiver method and the recently introduced vertical source-receiver time domain configuration. The problem is addressed from an analytical stand point, i.e. by analyzing closed form solutions of the 1D spatial and spectral distribution of the fields, and numerically, from 1D inversion of synthetic datasets as well as from 2D simulations of the response of finite lateral extent reservoirs. The 1D analysis demonstrates that the far offset measurement of the standard CSEM has more sensitivity to the presence of the resistive layer than the vertical source-receiver time domain measurement done at close offsets from the source. Closed form solutions derived for the *guided mode* of the fields yields increasing sensitivity of the standard CSEM configuration for thin resistors and increasing offsets from the source. The *image term* solution for the fields observed in the near offset vertical source-receiver configuration yields increasing sensitivity with decreasing frequency, i.e. towards the late times of the measurement. For the simplified single layer model a threshold offset is establish beyond which the standard CSEM method is more sensitive. However for a more realistic setting of a finite extent 2D reservoir this report shows that the guided mode driving the far offset sensitivity is only dominant for wide enough targets. The vertical source receiver is more sensitive to smaller targets, where the guided mode does not develop, and it has better resolution to the lateral extent of the reservoirs.

INTRODUCTION

In marine CSEM hydrocarbon exploration an electromagnetic (EM) source is used to excite the subsurface by radiating low frequency energy and simultaneously record the resulting EM fields as a function of time and space. The marine CSEM HED method (henceforth designated J_xE_x) consists of a towed (e.g. 300 m) antenna emitting harmonic (e.g. 0.25 Hz fundamental) energy, and an array of stationary receivers recording the fields in the sea bottom (T. Eidesmo et al., 2002). This method is widely used, however a vertical source-receiver time domain measurement (henceforth designated J_zE_z) has emerged as an alternative method, which could discriminate deep resistive targets even at very close source receiver offsets (Barsukov et al., 2007). This report addresses the question of sensitivity of each technique to the properties of a resistive target embedded in a more conductive host.

It has been shown (Weidelt (2007), Loseth (2007)) that the response of a resistive layer at far offsets is due to the so called *guided mode* of the fields. The resistive target channels energy preferentially in the radial direction, as it leaks out to the more conductive surrounding. The response of the layer is determined from the spatial falloff of the fields escaping the resistive channel. In the vicinity of the source instead, the fields are better described as a superposition of image terms, i.e., due to the dominant dipolar component of the charge density induced on the boundaries of the layer (Cuevas and Alumbaugh, 2009). The question becomes which mode provides better sensitivity and resolution, and does the analysis hold when the target of interest has a finite lateral extent?

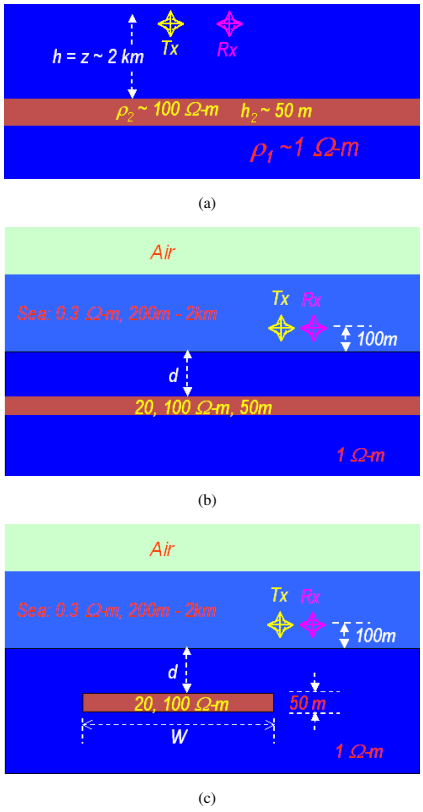

Figure 1: Canonical (a) single resistive layer model, (b) 1D model and (c) 2D model.

In this work the problem of comparing the sensitivity of each technique to the properties of the resistive body is approached both from an analytical perspective, deriving closed form solutions for the sensitivity to the properties of a resistive layer embedded in a whole space (fig. 1(a)), and numerically, analyzing 2D simulations as well as 1D inversion results for the response of the models described in fig. 1(c) and fig. 1(b) respectively.

CLOSED FORM SENSITIVITY

Consider the system in fig. 1(a): a resistive thin layer (σ_2, h_2) embedded in a homogeneous wholespace ($\sigma_1 > \sigma_2$), and an electric dipole source at $z = -h$, above the layer. The response at far offsets from the source yields a horizontal electric field

$$E_x = \frac{Ids}{4\pi\sigma} A_{10} e^{-u_{1,0}(h-z)-i\lambda_0 r} \left(\frac{2i}{\pi\lambda_0 r}\right)^{1/2} \left[\frac{2i\lambda_0}{r} - \lambda_0^2\right]$$
$$A_{10} \sim \frac{2\pi i}{\rho_2 h_2 \sigma_1} \frac{\lambda_0^2 - k_1^2}{\lambda_0^2}; \quad u_{1,0}^2 = \lambda_0^2 - k_1^2; \quad (1)$$

which is the dominant (Weidelt (2007), Loseth (2007)) contribution of the residue of the *TM* mode integration kernel at the position of the resistive layer pole, λ_0. Cuevas et al. (2009a) shows that λ_0 is a function of the $\rho_2 h_2$ product, thus the sensitivity to the layer properties is readily obtained by estimating the relative change of the field with respect to $\rho_2 h_2$, i.e.

$$\left|\frac{1}{E_x}\frac{\partial E_x}{\partial(\rho_2 h_2)}\right| \sim \frac{2^{3/4} r}{\sigma_1(\rho_2 h_2)^2} \left|\frac{2\sqrt{2} - \rho_2 h_2 \sigma_1 k_1 (1+i)}{(\sqrt{2} - \rho_2 h_2 \sigma_1 k_1 (1+i))^{1/2}}\right| \quad (2)$$

representing the dominant $e^{-i\lambda_0 r}$ behavior of the guided mode, which also describes the far offset limit of the vertical source-receiver configuration (Cuevas et al., 2009b). The r dependence suggests a loss of resolution with decreasing distance. However Cuevas and Alumbaugh (2009) show that the guided mode concept does not hold at near offsets, where the fields are rather described by a superposition of image terms. In this regime the E_z field is approximated ($\sigma_1 \gg \sigma_2$, $h_2^2 k_1^2 \ll 1$) by the series

$$E_z = \frac{Ids}{4\pi\sigma_1} \sum_{n=0}^{\infty} \frac{-i\pi(2 - u_{1,n}\rho_2 h_2 \sigma_1)}{u_{1,n}(\rho_2 h_2 \sigma_1 u_{1,n} + 2)} \lambda_n^3 k_2 e^{-u_{1n}(h-z)}$$
$$u_{1n}^2 = \lambda_n^2 - k_1^2; \quad \lambda_n = -ik_2(2n+1)\frac{\pi}{2} \quad (3)$$

which best holds (Cuevas and Alumbaugh, 2009) towards the low frequency, i.e.late time of interest in the vertical source receiver configuration. Using (3) the sensitivity functions for changes in layer thickness and conductivity are

$$\frac{1}{E_z}\frac{\partial E_z}{\partial h_2} = \frac{1}{h_2} \frac{2}{ik_1 a_n \sigma_1^{1/2} h_2 \rho_2^{1/2}} \quad (4)$$

$$\frac{1}{E_z}\frac{\partial E_z}{\partial \sigma_2} = \frac{1}{\sigma_2}\left(\frac{3}{2} - ia_n k_2 (h-z) + \frac{1}{ik_1 a_n \sigma_1^{1/2} h_2 \rho_2^{1/2}}\right) \quad (5)$$

where $a_n |k_1| \sigma_1^{1/2} h_2 \rho_2^{1/2} \gg 1$ holds for the higher order terms of the series, those which are more important for the lower frequencies (late times).

In the $J_x E_x$ method sensitivity benefits from increasing offsets, while at near offsets $J_z E_z$ benefits from decreasing frequencies, i.e towards the late times. In both methods however, the signal will drop below the background noise floor, in one case from geometrical attenuation of the signal and in the other due to the increasing amplitude of natural fields with decreasing frequency, or in time domain the decay of the fields below the measurement noise.

For $J_x E_x$, sensitivity depends inversely on $\rho_2 h_2$, but it is gained back by going out to farther distances, and higher frequencies ($\omega^{1/4}$ in eqn.2). For $J_z E_z$ sensitivity depends inversely on h_2, but directly on ρ_2 instead. Towards the late times (decreasing frequency) sensitivity to changes in layer thickness increases as $\omega^{-1/2}$, but sensitivity to changes in conductivity asymptotes in (5) to $3\rho_2/2$. Using this asymptotic limit, for a fixed h_2 and assuming low enough frequency such that frequency dependence in (2) is negligible, then the ratio of the sensitivity to changes in conductivity between $J_x E_x$ and $J_z E_z$ is greater than unity for measurements done at offsets exceeding $r_0 = 2\sigma_1 \rho_2 h_2$ (e.g. $\rho_2 = 50$ Ω-m, $h_2 = 50$ m, $r_0 = 5$ km), beyond this threshold the channeling effect of the guided mode dominates.

1D INVERSION ANALYSIS

Using the model described in fig. 1(b), time and frequency domain datasets were obtained from 1*D* simulations, and in turn inverted using a standard Gaussian-Newton technique, together with a cooling scheme for determining the regularization parameter at each iteration. For a single frequency $J_x E_x$ (at 0.25 Hz) configuration, the dataset included 21 offsets from 1 to 8 km, while for fixed offset $J_z E_z$ ($r = 250$ m), 21 time points in the range of 0.1 to 10 sec were included. The noise floor was set to 10^{-15} V/m in the former case (Um and Alumbaugh, 2007), and 10^{-16} V/m in the latter, honoring the source moment of the $J_z E_z$ method. The inversion was performed using the same starting baseline (excluding the reservoir), as well as the same smoothing matrix in both the frequency and time domain. The inversion results for two scenarios of target depth, 1 km and 2 km are shown in fig. 2(a), 2(b) respectively. In both cases the model recovered using the time domain $J_z E_z$ configuration (blue) is very smeared out, and shifted to greater depth. On the other hand the 1D inversion results for the standard $J_x E_x$ configuration (red) very distinctly shows the presence of the layer and it places the peak value at the correct depth. This supports the theoretical analysis which indicated that configuration that measures the guided mode ($J_z E_z$) has greater resolution of the layer parameters than does the time domain vertical source-receiver technique, related to the *image term* dominating the close offset response.

2D SIMULATIONS

Consider the 2D model described in fig. 1(c): a laterally finite resistive reservoir (100 $\Omega - m$ and 50 m thick) is embedded in a more conductive (1 $\Omega - m$) background. Frequency and time domain numerical simulations were performed for the $J_x E_x$ and $J_z E_z$ measurement techniques of interest in this work. The response of the model is analyzed for various reservoir's width: 1D, 1,2, 4, an 6 km, and shallow (1 km) and deep (2 km) target depth. The detectability of the reservoir is evaluated

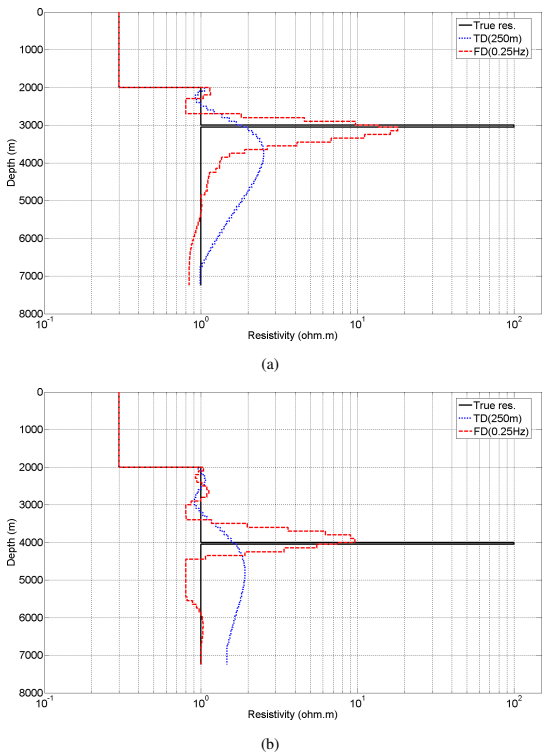

Figure 2: 1D inversion for a (a) shallow (1 km) and (b) deep (2 km) resistive layer. True model: black, J_xE_x: red, J_zE_z: blue.

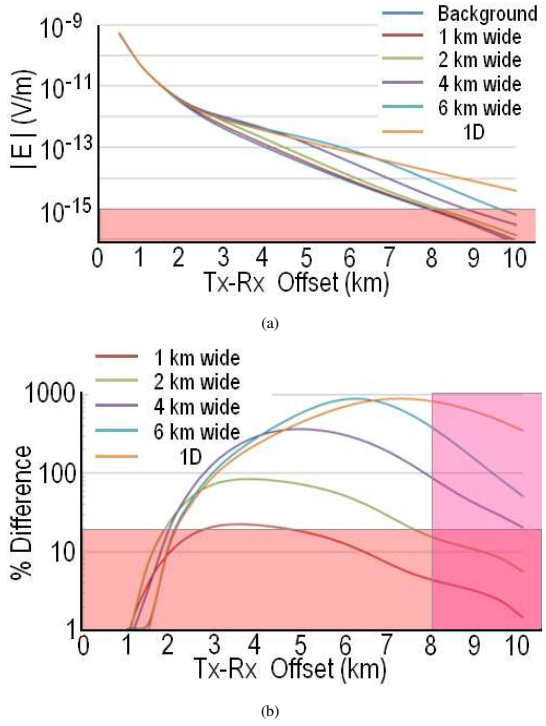

Figure 3: 2 km water depth, 1 km target depth, J_xE_x configuration. (a) Field amplitude (b) percent anomaly.

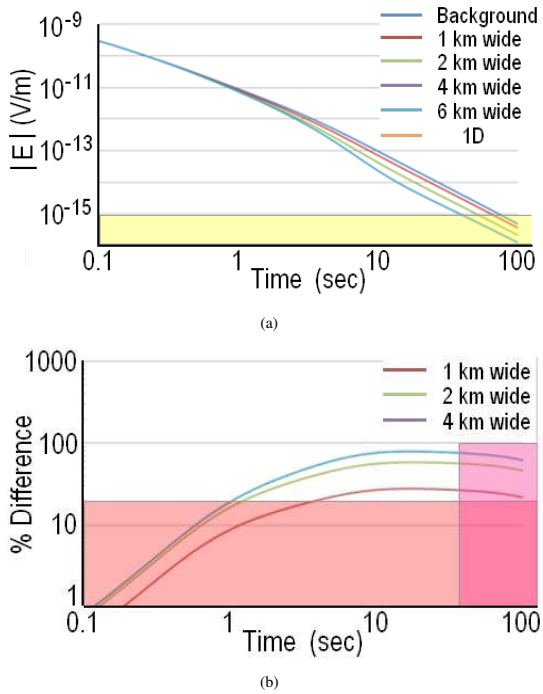

Figure 4: 2 km water depth, 1 km target depth, J_zE_z configuration. (a) Field amplitude (b) percent anomaly.

from the anomalous response produced by the presence of the reservoir, i.e. the relative change of the fields with respect to those observed in the background 1D model. The results for a deep water (2 km) shallow target (1 km) scenario are shown in fig. 3(a)- 3(b) for J_xE_x and in fig. 4(a)- 4(b) for J_zE_z. Evidently the anomaly observed in the J_xE_x configuration (fir. 3(b)) is far greater than that of J_zE_z (fig. 4(b)), in particular for the widest (6 km) reservoir. However while the anomaly produced by the smallest (1 km) reservoir drops below detectable levels in the J_xE_x method, it appears to remain detectable in the later times (> 10 sec) of J_zE_z.

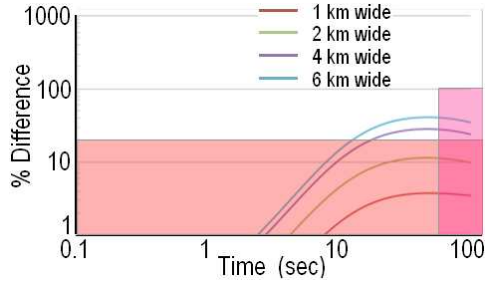

Figure 5: 2 km water depth, 2 km target depth: J_zE_z percent anomaly.

The offset for the J_xE_x plots is defined in common mid-point scheme, centered above the middle of the reservoir. In this case it is important to notice the *excess response*, above that of the 1D reservoir (orange curve), observed for offsets on the order of the target's width. The excess field is due to the en-

ergy flowing out of the resistive body developing the guided mode. The channeling effect appears to require a minimum target width to develop, below which the effect of the *image term* detected by the close offset J_zE_z method dominates. Furthermore the J_zE_z remains sensitive even in the deep target (2 km) scenario (fir. 5), where the J_xE_x configuration fails to provide measurable anomalies. Lateral resolution to the presence of the reservoir appears to be an strength of the J_zE_z configuration. Indeed fig. 6(b) shows the relative magnitude of the field with respect to those observed above the center of the 4 km wide reservoir. Great variations appear as the J_zE_z devise traverses over the edge of the target, but a smoother transition is obtained for the equivalent exercise for J_xE_x (fig. 6(a)).

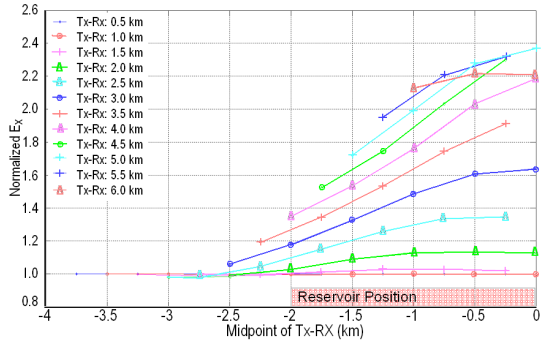

(a)

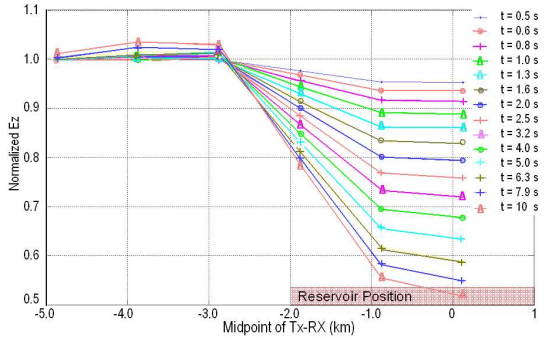

(b)

Figure 6: Lateral sensitivity of (a) J_xE_x and (b) J_zE_z.

For the different scenarios which were explored in this paper the chart in fig. 7 summarizes the detectability of each technique. The vertical axis describes the target of interest. The horizontal axis describes the ratio between the anomaly observed with each method, with the positive range reserved for deep water models (2 km), and the negative for shallow water models (200 m). Thus ratio values within ± 1 (dashed line) represent scenarios where J_xE_x is more sensitive. This is clearly the case for the wider reservoir (6 km) at depths shallower than 3 km. The color code constrains the detectability of the target using the J_zE_z configuration, in relation to the measurement noise floor. Thus although ratio values outside the ± 1 range (J_zE_z sensitivity) dominate for the shallow water scenarios, the anomalies for deeper and smaller (< 4 km) targets drop below 20 % of the measurement noise floor, rendering the ability to make the measurement a more challenging issue. For deeper (2 km) and wider targets (≥ 4 km) the J_zE_z has better sensitivity and it also provides a measurable anomaly.

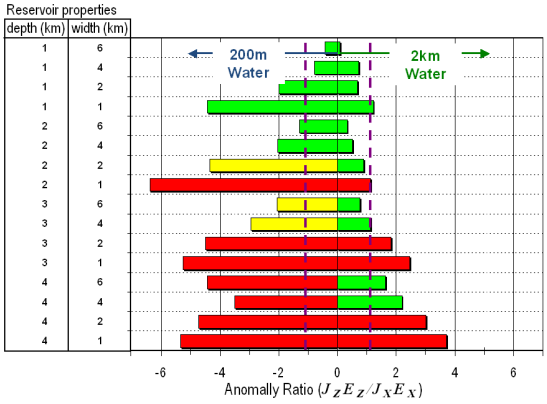

Figure 7: Anomalous response of 2D target using J_xE_x vs J_zE_z methods. Green: J_zE_z Anomaly $> 20\%$, measurable at times less than noise floor time. Yellow: J_zE_z Anomaly $> 20\%$, measurable at noise floor time. Red: J_zE_z Anomaly $< 20\%$ and or measurable later than noise floor time.

CONCLUSIONS

In this work a comparison is shown for the sensitivity to the presence of a resistive target of two marine CSEM measurement methods: frequency domain J_xE_x and time domain J_zE_z. From an analytical perspective it is shown that at far offsets from the source changes in the field with $\rho_2 h_2$ are proportional to the radial distance, and inverse to $\rho_2 h_2$. For the near offset J_zE_z instead, sensitivity increases with decreasing frequencies as $\omega^{-1/2}$, and it depends inversely on σ_2 and h_2 instead. In comparison resolution to thin resistive layer is better obtained at far offsets and using the J_xE_x measurement, which benefits from the radial falloff of the guided mode phenomena developing at far offsets from the source. This conclusion is supported by 1D inversions using both techniques, where it is evident that the resistive layer is better resolved using such a technique. However a more realistic 2D analysis suggests that as the lateral extent of the reservoir decreases, the guided mode disappear but the effect of the image terms remains. As a consequence choosing the method that better detects the presence of the 2D resistive body depends on the target's depth and lateral extent. This study shows that the J_xE_x mode provides better sensitivity and resolution to the presence of wide targets (width $\gg$ depth). Conversely the J_zE_z provides better sensitivity as the target's lateral extent becomes comparable and smaller than its depth. In addition the J_zE_z mode appears to provide better lateral resolution, although further 2D (and 3D) inversion analysis is needed to support this observation.

ACKNOWLEDGMENTS

The authors thank Schlumberger for permission to publish this work.

EDITED REFERENCES

Note: This reference list is a copy-edited version of the reference list submitted by the author. Reference lists for the 2010 SEG Technical Program Expanded Abstracts have been copy edited so that references provided with the online metadata for each paper will achieve a high degree of linking to cited sources that appear on the Web.

REFERENCES

Barsukov, P., F. E, and S. B., 2007, A method for hydrocarbon mapping and apparatus for use when performing the method: Patent WO 2007/053025 A1.

Cuevas, N. and D. Alumbaugh, 2009, Near offset response of the resistive layer to a vertical electric dipole excitation: SEG Expanded abstract, 28, 794.

Cuevas, N., D. Alumbaugh, and H. F. Morrison, 2009a, Analytical expressions for the electromagnetic fields for a 1d resistive layer in a conductive wholespace system: EAGE Expanded abstract.

Cuevas, N., D. Alumbaugh, and H. F. Morrison, 2009b, Analytical expressions for the electromagnetic fields for a 1d resistive layer in a conductive wholespace system: Submitted to Geophys. Prosp.

Loseth, L. O., 2007, Modelling of controlled source electromagnetic data.: PhD thesis, Norwegian University of Science and Technology.

T. Eidesmo, S. Ellingsrud, L. M. MacGregor, S. Constable, M. C. Sinha, S. Johansen, F. N. Kong, and H. Westerdahl, 2002, Sea Bed Logging (SBL), a new method for remote and direct identification of hydrocarbon filled layers in deepwater areas using controlled source electromagnetic sounding: First Break, **20**, 144–152.

Um, E., and D. Alumbaugh, 2007, On the physics of the marine controlled-source electromagnetic method: Geophysics, **72**, no. 2, WA13–WA26, doi:10.1190/1.2432482.

Weidelt, P., 2007, Guided waves in marine csem: Geophysical Journal International, **171**, no. 1, 153–176, doi:10.1111/j.1365-246X.2007.03527.x.